EVALUATION OF LASER SURFACE IRRADIATION ON THE MODE I FRACTURE TOUGHNESS OF COMPOSITE JOINTS WITH CFRP ADHERENDS

Ran Tao[1], Marco Alfano[2] and Gilles Lubineau[1]

[1] King Abdullah University of Science and Technology (KAUST), Physical Sciences and Engineering Division, COHMAS laboratory, Thuwal, Saudi Arabia, ran.tao@kaust.edu.sa, gilles.lubineau@kaust.edu.sa, cohmas.kaust.edu.sa
[2] University of Calabria, Department of Mechanical, Energy and Management Engineering, P. Bucci 44C, Rende, Italy, marco.alfano@unical.it, www.unical.it

Keywords: Composite laminates, Adhesive joints, Laser irradiation, Fracture toughness

ABSTRACT

Secondary bonding of cured carbon fiber reinforced polymer (CFRP) laminates using structural adhesives has attracted great attention from the aerospace industry. The most important process step to achieve reliable joints is the execution of a proper surface pre-treatment. In this paper, pulsed CO_2 laser irradiation was employed to increase the mode I fracture toughness of CFRP adhesive joints. In order to evaluate the effect of laser irradiation on CFRPs, surface chemistry and morphology were assessed through XPS and SEM analyses. The mode I fracture toughness was determined using the DCB specimen and fracture surfaces were surveyed using optical and SEM.

1 INTRODUCTION

Three main techniques are currently available to join carbon fiber reinforced polymer (CFRP) thermoset composites: co-curing, co-bonding and secondary bonding [1]. Secondary bonding has extensive applications due to its flexibility to bond large and complex parts. Instead of adding extra rivets or drilling holes, adhesively bonded composite joints achieve light weight and uniform stress distributions within the joint bondline. Despite the advantages offered by secondary bonding, most primary load-bearing structural joints still rely on mechanical fasteners. This is due to the lack of confidence in the reliability of composite/adhesive interfaces.

Surface pre-treatments are critical in this respect and play a very important role on the joint fracture toughness [2]. Two main pathways are available to enhance the fracture toughness: tailor surface chemistry to promote chemical bonding [3] and modify surface morphology to trigger the mechanical interlocking [4-8].

Peel plies are commonly used when fabricating CFRP laminates and create a textured, clean and active surface for adhesive bonding. However, release agents within the peel ply very often lead to surface contamination, and thus lower the bond toughness [9]. State of the art controllable and reproducible surface preparation techniques are necessary to prevent surface contamination and achieve high fracture toughness of adhesive bonded composite joints [1]. Among various techniques, pulsed laser irradiation has the advantage to achieve a fast and controllable surface modification [10-12]. Using pulsed laser irradiation, surface chemistry and morphology were simultaneously modified [13] and controllable surface patterns, able to enhance fracture toughness, could also be obtained [14]. On the other hand, the protruding carbon fibers due to complete surface epoxy removal was shown to introduce detrimental effects on bonding [15]. Therefore, it is very important to carefully select laser-processing parameters and evaluate the obtained surface conditions in order to increase fracture toughness.

In this study, the effect of pulsed CO_2 laser irradiation on the mode I fracture toughness of CFRP/epoxy joints was evaluated. First, elemental atomic concentration and crystalline order of carbon materials were probed using X-ray photoelectron spectroscopy (XPS) and Raman spectroscopy. Next, surface profiles were obtained by a contact profilometer to assess the effect of

laser processing parameters on the resulting surface morphologies. Finally, double cantilever beam (DCB) tests were carried out to investigate the mode I fracture toughness of the joints.

2 MATERIALS AND METHODS

2.1 Material

The substrate materials used in present work were aerospace grade unidirectional carbon fiber prepregs made up of toughened epoxy resin and carbon fibers (HexPly T700/M21, Hexcel, Stamford, CT, USA) with the nominal fiber volume of 56.9%. Unidirectional carbon fiber reinforced laminates ($[0^o]_8$) were fabricated by compression molding. The curing cycle of the laminate was conducted as follows. Full vacuum (1 bar) was firstly applied to the whole stack in order to tackle air entrapment and the formation of voids in the final laminate. Afterward, a (7 bar) gauge pressure was applied by a hydraulic hot press machine (Hydraulic presses, Pinette Emidecau Industries, Chalon sur Saone, France) with the heating rate of 3^oC/min and then held at 180^oC for 120 min. Finally the laminate was cooled down at 3^oC/min.

The adhesive selected for bonding cured CFRP substrates was a two-component room temperature curing epoxy (Araldite 420 A/B, Huntsman, Salt Lake City, UT, USA). It is a structural adhesive with very high shear and peel strengths which bonds materials such as metals, composites and thermoplastics. The basic mechanical properties of the adhesive provided by the manufacturer through tensile tests are as follows: Young's modulus, E=1.5 GPa; elongation at break ε_f=4.6%; tensile strength, σ_f=29 MPa [8].

2.2 Surface treatments

Various surface pre-treatment strategies were deployed prior to adhesive bonding. The baseline preparation was represented by the application of a Teflon film (**T**) to obtain a nominally flat interface for subsequent pulsed laser irradiation. The prepreg surface was initially covered by a Teflon film during curing and before adhesive bonding the film was removed.

Pulsed laser irradiation was then employed to achieve efficient and controllable surface treatments using a 10.6 μm CO_2 laser (PLS6.75 Laser Platform, Universal Laser Systems, NY, USA). Different surface modifications were imparted by controlling adjustable laser process parameters. Actual depth and quantity of affected material mainly depended on pulse fluences (F_p) calculated by the following equation,

$$F_p = I_p\, t_p = W_{ave}/(f\, A_s) \tag{1}$$

where I_p represents the laser irradiance, t_p is the laser pulse duration, f (=v PPI) is the pulse frequency, W_{ave} is the average pulse power and A_s (=$\pi d^2/4$) is the spot size. Several parameters remained unchanged for different treatments, such as the traveling speed v=500 mm/s, the pulse number per inch PPI=1000 and the laser spot diameter d=200 μm.

Four treatments featuring different pulse fluences were assessed by varying the average power W_{ave} (Table 1). Two developed treatments were represented by uniform laser irradiation to eliminate surface contaminations (**TLC**) or remove the surface epoxy (**TLA**). However, to improve surface texturing, laser trenches parallel to the fiber direction (**LTX**) were applied to the T surface. In the forth treatment, uniform laser cleaning (TLC) was employed prior to surface texturing (**LTX***).

Surface treatment	TLC	TLA	LTX
Pulse fluence (J/cm^2)	1.2	3.6	9.1

Table 1: Surface treatments and corresponding laser fluence.

After pulsed laser irradiation, all surfaces were degreased in ultrasonic bath in acetone for 10 minutes and then dried in the oven at 50^oC for 25 minutes before applying adhesives.

2.3 XPS and Raman analyses

Chemical element analyses were performed with X-ray photoelectron spectroscopy (XPS) (Amicus, Kratos Analytical Ltd, Manchester, UK) to quantify surface chemistry modifications after different pulse laser irradiation. Global surveys were performed on selected surfaces with 200 ms dwell time and 30 scans of the wide range (binding energy range from 1200 to 0 eV) under a vacuum (10^{-6} mbar). Measurements were performed in hybrid mode using electrostatic and magnetic lenses.

A Raman spectrometer (LabRAM Aramis, Horiba Scientific, Kyoto, Japan) was employed and the range of 1100-1800 cm^{-1} was explored. A diode-pumped solid-state (DPSS) laser with wavelength of 473 nm was used as the excitation source. The laser power on the sample surface was fixed at 0.07 mW to avoid the heating effects on the sample. A 50x long work distance lens with numerical aperture (N.A.) of 0.5 was used to focus laser and collect scattered lights. The exposure time on single spot was 15 s x 15. The D-band and the G-band of the carbon material are respectively at 1350 and 1580 cm^{-1}. The relative intensity (D/G) between the D and the G bands is known to be a good indicator to identify crystalline order of carbon materials, providing useful information about the phases and structural defects in carbon materials [17,18].

2.4 Surface morphology characterization

The evolution of surface morphology was analysed qualitatively under a scanning electron microscope (SEM) (Quanta 600, FEI, CA, USA) using secondary electron imaging, and quantitatively using a contact profilometer (Dektak 150 Surface Profiler, Veeco, New York, USA) (gage length of 3 mm and 0.1667 μm resolution). Six scans were carried out in both parallel and perpendicular to the fiber direction. The absolute roughness was determined in both directions as the indicator of the average height of the peaks and valleys over the surface to quantify the morphology:

$$R_a=(1/n)\ \Sigma|y_i-y_{mean}| \tag{2}$$

where n is the number of sampling points of each scan, y_i is the detrended height of the surface profile and y_{mean} is the average value of all y_i values.

2.5 Mechanical DCB tests

Mode I delamination fracture tests were conducted using double cantilever beam (DCB) specimens with various surface treatments according to ASTM D5528-13 standard [16]. Cured unidirectional CFRP laminates ($[0^o]_8$) were adhesively bonded using Araldite 420 A/B. After a chosen surface treatment, the adhesive was applied uniformly to the surface. A nonadhesive insert (60 mm long, 40 μm thick according to the ASTM standard [16]) was put between two substrates, serving as a delamination initiator. Two copper wires (100 μm diameter) were used as the spacer to control the thickness of the adhesive layer. Bonded joints were cured at the room temperature for 12 hours and were then cut into 250 x 20 x 4 mm^3 slices. Opening peel forces were applied to DCB specimens through loading blocks and by controlling the crosshead displacement at a speed of 5 mm/min using a universal testing system (Instron 5882, Instron, Massachusetts, USA), while the load and crack length were recorded. The crack propagation was optically observed *in situ* by a Cannon EOS-1Ds camera (with the resolution of 5616 x 3744) to track the delamination crack growth during testing though crack length gages bonded to the specimen edge. The test pictures were employed in order to track the evolution of crack size as a function of the opening displacement and applied load. The mode I delamination fracture toughness (G_{Ic}) was then calculated out of at least five specimens of each surface treatment according to the procedures and the recommendations provided by the standard ASTM D5528-13 [16]. The compliance calibration method (CC) was used in this work to calculated G_{Ic},

$$G_{Ic}=nP\delta/2ba \tag{3}$$

where P is the applied load, δ is the load point displacement, b is the specimen width, a is the delamination length and n is the compliance calibration term. In present work n was determined by generating a least squares plot of the logarithmic compliance (log C) as a function of the logarithmic crack length (log a).

The optical imaging and the secondary electron analysis using SEM were carried out to probe the fractured surfaces after mechanical tests and highlight failure modes of the adhesive within the substrates.

3 RESULTS AND DISCUSSIONS

3.1 XPS survey of treated surfaces

XPS analyses were performed and the atomic percentage concentrations of surface elements are shown in Table 2. The content of fluorine (F) element, which comes from the Teflon film, was reduced after the removal of the surface epoxy. The results given in Table 2 show that the F element decreases from T to TLC surfaces and vanishes in TLA, LTX and LTX*. However, compared to previous work [15], limited atomic concentration of F was reported in the XPS survey. New elements such as sodium (Na) and phosphorus (P) appeared in TLA, LTX and LTX* surfaces, which are additives coming from the underlying bulk material and which are typically used in aerospace composites [19,20]. However, none of previous related works claimed that additive elements (*i.e.* Na or P) affected composite bonding. Other elements, like N and S, remained unchanged among all surface treatments. It has been recently reported that silicon is a critical surface contaminant. Analyses carried out on the very same composite laminates employed herein highlighted that Si can significantly lower the adhesion when its atomic concentration is greater than 5% [21].

Surface treatments	C	O	F	Si	Other (N, S, Na, P)
T	67.1	18.8	5.2	5.3	balance
TLC	69.4	17.1	2.3	2.5	
TLA	61.5	25.9	0	2.5	

Table 2: XPS measurement of different treatments.

As previously described, Raman spectra were determined and are reported in Figure 1(a). However, direct comparison of intensity values can be affected by Raman measurement errors, *e.g.* laser beam focus, intensity fluctuations, the orientation of the sample relative to the laser beam. Therefore, intensity ratios I_D/I_G were calculated to identify the crystalline order of carbon materials and are reported in Figure 1(b).

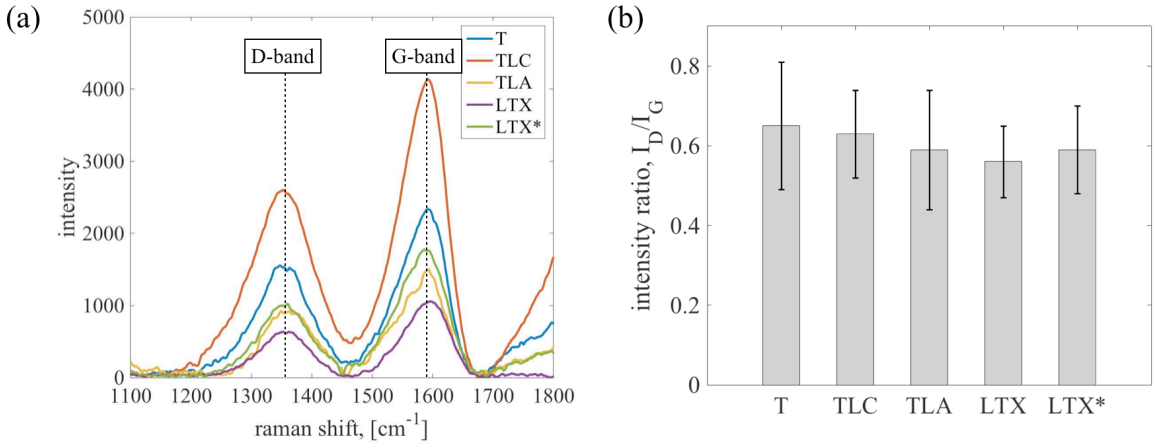

Figure 1: (a) Raman spectra of various surface treatments; (b) intensity ratio between D-band and G-band of carbon materials.

Since no significant differences were observed in the intensity ratio I_D/I_G, it is inferred that all treated surfaces feature the same chemical structure of carbon materials, indicating the absence of significant variation in the amount of structural defects in carbon fibers.

3.2 Surface morphology indicators

Treated surfaces were observed under SEM to have qualitative understanding of induced morphological modifications, see Figure 2. The baseline T surfaces demonstrate a flat morphology with the imprinted texture from the Teflon film. TLC surfaces have partially exposed fibers and display the appearance of micron-sized particles, which might arise from the burned epoxy, while TLA surfaces demonstrate fully exposed carbon fibers because of the removal of the surface epoxy. The exposure of carbon fibers thereby leads to anisotropic surface morphologies. Finally, textured surfaces were obtained by means of trenches as shown in the SEM images of LTX and LTX* treatments. Notice that the spacing between consecutive trenches was set equal to 500 μm.

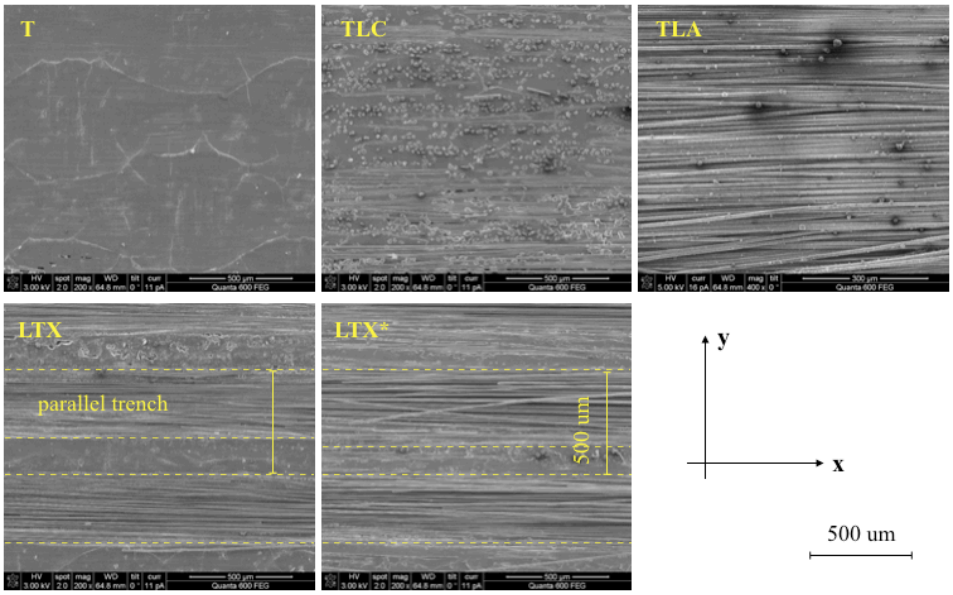

Figure 2: Morphology of various surface treatments under SEM imaging.

The surface profiles, and the corresponding absolute roughness (R_a), shown in Figure 3 display the anisotropy of the surfaces treated by means of the pulsed CO_2 laser irradiation. T surfaces have relatively low roughness, while TLC and TLA have rougher surface sharing similar R_a roughness in the two orthogonal directions. The surfaces of LTX and LTX* have multiple roughness values since different treatments are combined to achieve patterned interfaces. On LTX surfaces, R_{ax} within trenches is 2.35±0.56 μm, while outside trenches is the same as that of T surfaces, *i.e.*, 3.15±0.74 μm. Similarly, in LTX* surfaces, R_{ax} within trenches is 3.67±1.06 μm while outside trenches is the same as that of TLC surfaces, *i.e.*, 3.48±0.89 μm. In any case, both LTX and LTX* have the highest surface absolute roughness along the y direction.

3.3 Fracture toughness of DCB samples

The typical load response of DCB tests is shown in Figure 4 (a). The response curve from the DCB test consists of an initial linear elastic increasing region, which corresponds to the bending of the beam with the initial crack length, followed by a crack propagation region, which has a decreasing load response. Load and unloading cycles were employed during tests to reduce as much as possible unstable crack growth. Young's modulus (E=125 GPa) of UD laminates was obtained from the slope of the elastic region, and was consistent with nominal modulus of the employed prepreg. The typical CC calibration (Eq. 3) is shown in Figure 4 (b).

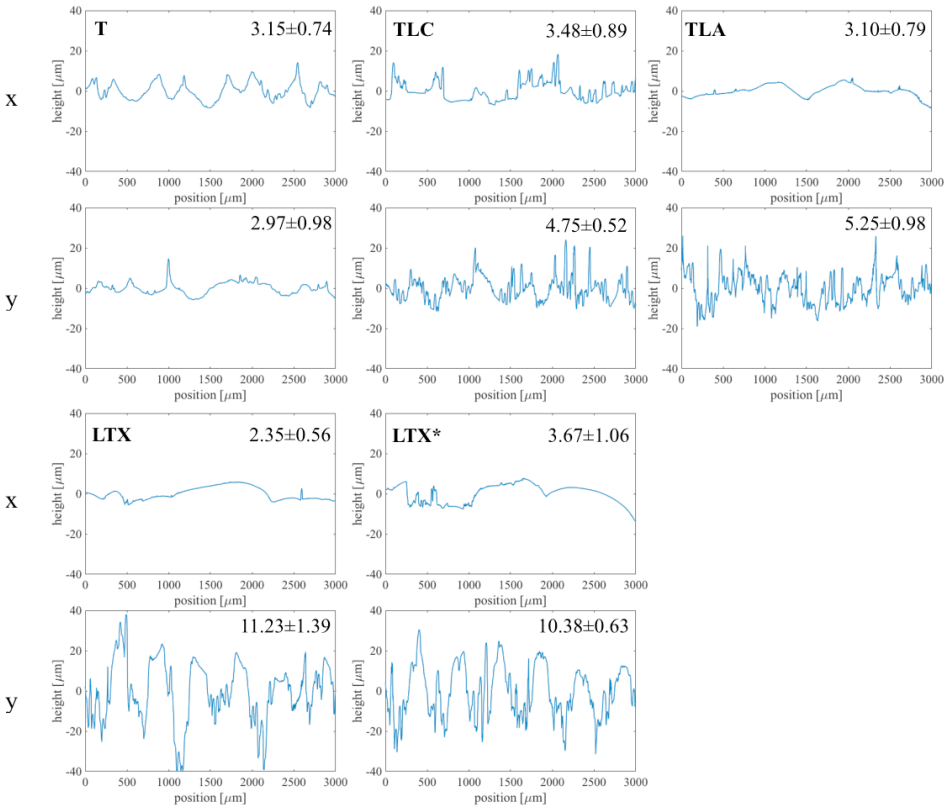

Figure 3: Roughness of various surface treatments. Fiber orientation and crack growth are in the x-direction. The average R_a in the plots is given in [μm].

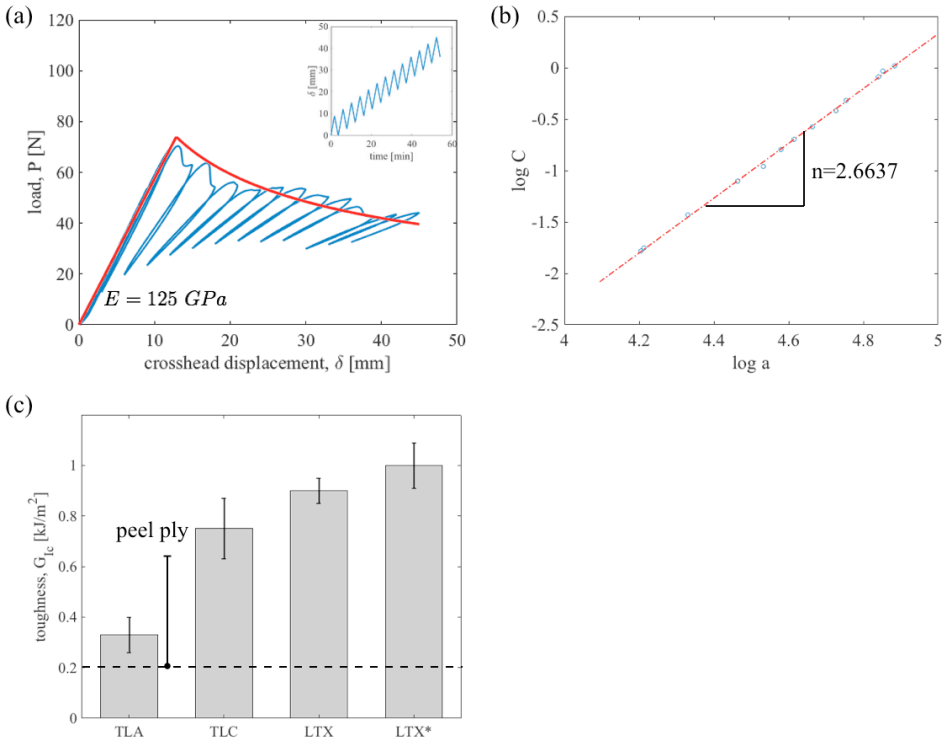

Figure 4: (a) Typical load-displacement response; (b) compliance calibration for DCB tests; (c) obtained values of fracture toughness as a function of surface conditions.

The mode I fracture toughness (G_{Ic}) results are reported in Figure 4 (c). Calculation of the fracture toughness of the baseline T surfaces was not possible, since catastrophic failure occurred during tests. Thus, fracture toughness of T surfaces is not reported in Figure 4 (c). Compared to a standard treatment using the peel ply, which is represented by the dash line in Figure 4 (c), pulsed CO_2 laser irradiation demonstrates the ability to largely enhance fracture toughness.

Local failure modes were qualitatively observed through both optical and high resolution SEM fracture surfaces shown in Figure 5. TLC fracture surfaces exhibit a combined interfacial and cohesive failure, and thus TLC surfaces have higher toughness. TLA surfaces have relative low fracture toughness, demonstrating mainly interfacial failure. Although LTX surfaces also experience mainly interfacial failure, higher fracture toughness is achieved because of the increased contact area. Furthermore, LTX* fracture surfaces showed extensive cohesive failures and fiber bridging identified by broken fibers on surfaces.

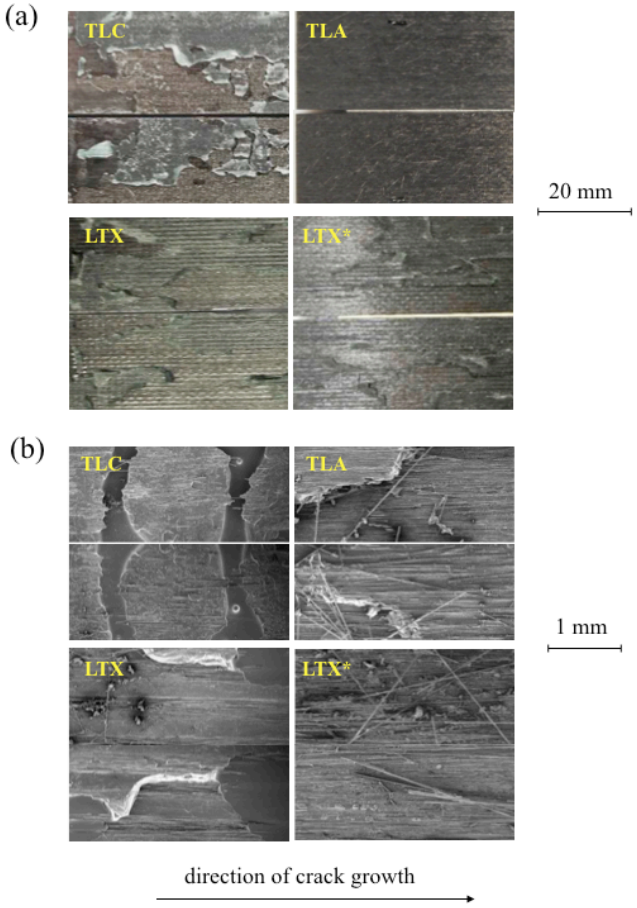

Figure 5: Fracture surfaces, (a) optical observation and (b) SEM imaging.

Finally, Figure 6 reports the obtained values of fracture toughness as a function of fracture toughness G_{Ic}' calculated using the law of mixture,

$$G_{Ic}' = G_{Ic}^{1}\varphi_1 + G_{Ic}^{2}\varphi_2 \quad (4)$$

where G_{Ic}^{1} and G_{Ic}^{2} are the fracture toughness of two treatments, respectively, φ_1 and φ_2 are corresponding area fraction. A representative square is extracted and shown as the blue region in Figure 6. Since trenches develop along the x-direction, the width ratio of different treatment regions gives the area fraction. Considering that the pattern spacing is 500 μm, 260 μm width of trenches indicates an area fraction 52%.

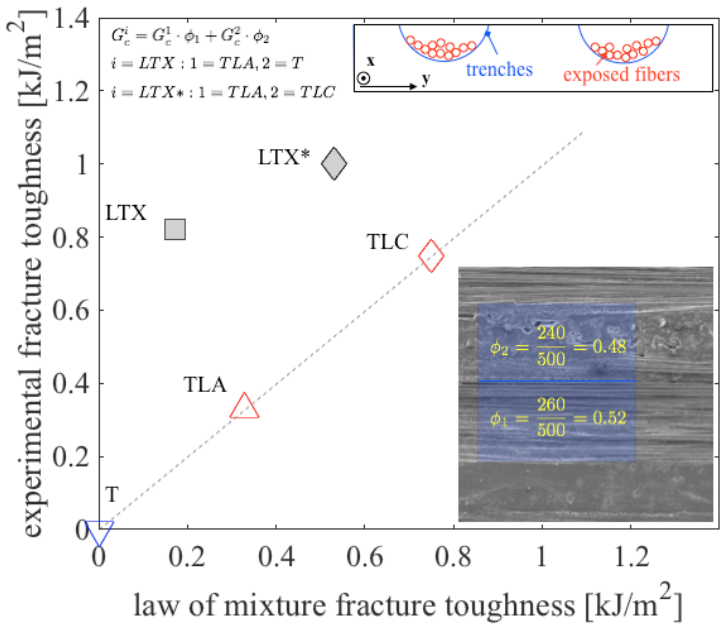

Figure 6: Fracture toughness of patterned treatments compared with the toughness calculated from the law of mixture.

Both patterned and uniform treatments are plotted in Figure 6. Uniform treatments T, TLC and TLA all locate on the dashed line, representing same experimental toughness as calculated toughness using the law of mixture. However, patterned treatments LTX and LTX* deviate from the prediction of the law of mixture. The enhancement of fracture toughness on LTX and LTX* surfaces should mainly come from the increased bonded area compared to the "flat" case, as the schematic shown in Figure 6. Furthermore, energy dissipation during fracture can be also elevated by promoted mechanical interlocking due to curved surface profile and the induced bridging effects associated to exposed carbon fibers.

4 CONCLUSION

In this study, the effect of pulsed CO_2 laser irradiation on the mode I fracture toughness of adhesively bonded CFRP joints was investigated. First of all, pulsed CO_2 laser irradiation with different pulse fluences were employed to realize different surface treatments. Next, elemental atomic concentration and crystalline order of carbon material were characterized by XPS measurements and Raman spectra. Then, the surface morphology was evaluated by SEM observations, contact profilometer scans and surface roughness R_a. Finally, the mode I fracture toughness was evaluated.

Results indicated that pulsed CO_2 laser irradiation could largely enhance the mode I fracture toughness of adhesively bonded CFRP joints. Both fluorine and silicone were proven to be surface contaminants and Si played a more critical role in lowering the adhesion when a critical atomic concentration is reached according to XPS surveys. While Raman spectra demonstrated that no significant variation in the amount of structural defects in carbon fibers. Pulsed laser irradiation efficiently eliminated surface contamination and promoted adhesive bonding, improving fracture toughness to higher values compared to the standard peel ply treatment. Patterned interfaces further enhanced fracture toughness. In particular, increased contact area and mechanical interlocking allowed to enhance energy dissipation, resulting in the deviation from the law of mixture. Therefore it is concluded that the surface treatments deployed in the present work promoted an increase of fracture toughness because of the elimination of surface contamination and morphology modifications.

ACKNOWLEDGEMENTS

The research reported in this publication was supported by funding from King Abdullah University of Science and Technology (KAUST).

REFERENCES

[1] T.A. Schmid Fuertes, T. Kruse, T. Körwien and M. Geistbeck, Bonding of CFRP primary aerospace structures and discussion of the certification boundary conditions and related technology fields addressing the needs for development, *Composites Interfaces,* **22**, 2015, pp. 795-808 (doi: 10.1080/09276440.2015.1077048).

[2] S.G. Prolongo, M.R. Gude, G. Del Rosario and A. Ureña, Surface pretreatments for composite joints: study of surface profile by SEM image analysis, *Journal of Adhesion Science and Technology,* **24**, 2010, pp. 1855-1867 (doi: 10.1163/016942410X507623).

[3] I. Jölly, S. Schlögl, M. Wolfahrt, G. Pinter, M. Fleischmann and W. Kern, Chemical functionalization of composite surfaces for improved structural bonded repairs, *Composites Part B: Engineering,* **69**, 2015, pp. 296-303 (doi: 10.1016/j.compositesb.2014.10.020).

[4] Q. Bénard, M. Fois and M. Grisel, Peel ply surface treatment for composite assemblies: Chemistry and morphology effects, *Composites Part A: Applied Science and Manufacturing,* **36**, 2005, pp. 1562-1568 (doi: 10.1016/j.compositesa.2005.02.012).

[5] W.S. Kim, I.H. Yun, J.J. Lee and H.T. Jung, Evaluation of mechanical interlock effect on adhesion strength of polymer/metal interfaces using micro-patterned surface topography, *International Journal of Adhesion and Adhesives,* **30**, 2010, pp. 408-417 (doi: 10.1016/j.ijadhadh.2010.05.004).

[6] H.T. Gao, X. Yang, P. Huang and K.W. Xu, Enhancement mechanism of super fine machining pattern on mechanical property of adhesion interface of Al alloy, *Physics Procedia,* **50**, 2013, pp. 288-292 (doi: 10.1016/j.phpro.2013.11.046).

[7] Y. Yukimoto, R. Matsuzaki and A. Todoroki, Effects of mixed-mode ratio and step-shaped micro pattern surface on crack-propagation resistance of carbon-fiber-reinforced plastic/adhesive interface, *Composites Part A: Applied Science and Manufacturing,* **69**, 2015, pp. 139-149 (doi: 10.1016/j.compositesa.2014.11.014).

[8] A.T.T. Nguyen, M. Brandt, A.C. Orifici and S. Feih, Hierarchical surface features for improved bonding and fracture toughness of metal-metal and metal-composite bonded joints, *International Journal of Adhesion and Adhesives,* **66**, 2016, pp. 81-92 (doi: 10.1016/j.ijadhadh.2015.12.005).

[9] J. Holtmannspötter, J.V. Czarnecki, M. Wetzel, D. Dolderer and C. Eisenschink, The use of peel ply as a method to create reproduceable but contaminated surfaces for structural adhesive bonding of carbon fiber reinforced plastics, *The Journal of Adhesion,* **89**, 2013, pp. 96-110 (doi: 10.1080/00218464.2012.731828).

[10] M. Alfano, G. Lubineau, F. Furgiuele and G.H. Paulino, On the enhancement of bond toughness for Al/epoxy T-peel joints with laser treated substrates, *International Journal of Fracture,* **171**, 2011, pp. 139-150 (doi: 10.1007/s10704-011-9636-4).

[11] M. Alfano, G. Lubineau, F. Furgiuele and G.H. Paulino, Study on the role of laser surface irradiation on damage and decohesion of Al/epoxy joints, *Journal of Adhesion Science and Technology,* **39**, 2012, pp. 33-41 (doi: 10.1016/j.ijadhadh.2012.03.002).

[12] K. Almuhammadi, L. Selvakumaran, M. Alfano, Y. Yang, T.K. Bera and G. Lubineau, Laser-based surface preparation of composite laminates leads to improved electrodes for electrical measurements, *Applied Surface Science,* **359**, 2015, pp. 388-397 (doi: 10.1016/j.apsusc.2015.10.086).

[13] E. Hernandez, M. Alfano, G. Lubineau and U. Buttner, Improving adhesion of copper/epoxy joints by pulsed laser ablation, *Journal of Adhesion Science and Technology,* **64**, 2016, pp. 23-32 (doi: 10.1016/j.ijadhadh.2015.10.003).

[14] F.L. Palmieri, J. Hopkins, C.J. Wohl, Y. Lin, J.W. Connell, M.A. Belcher and K.Y. Blohowiak, Laser surface preparation of epoxy composites for secondary bonding: optimization of ablation depth, 2015.

[15] Q. Bénard, M. Fois, M. Grisel and P. Laurens, Surface treatment of carbon/epoxy and glass/epoxy composites with an excimer laser beam, *International Journal of Adhesion and Adhesives,* **26**, 2006, pp. 543-549 (doi: 10.1016/j.ijadhadh.2005.07.008).

[16] ASTM Internat, Standard test method for mode I interlaminar fracture toughness of unidirectional fiber-reinforced polymer matrix composites, 2014.
[17] K. Almuhammadi, M. Alfano, Y. Yang and G. Lubineau, Analysis of interlaminar fracture toughness and damage mechanisms in composite laminates reinforced with sprayed multi-walled carbon nanotubes, *Materials and Design,* **53**, 2014, pp. 921-927 (doi: 10.1016/j.matdes.2013.07.081).
[18] L. Li, C. Liu, X. Zhang, G. Wu, M. Zhang, R.K.Y. Fu and Chu, P.K., Plasma-target surface interaction during non-equilibrium plasma irradiation at atmospheric pressure: Generation of dusty plasma, *Laser and Particle Beams,* **32**, 2013, pp. 69-78 (doi: 10.1017/S0263034613000888).
[19] S. Girish, K. Devendra and K.N. Bharath, Effect of sodium bicarbonate on fire behaviour of tilled E-glass reinforced epoxy composites, *IOP Conference Series: Materials Science and Engineering,* **149**, 2016, IOP Publishing, pp. 012-210.
[20] A. Toldy, B. Szolnoki and Gy. Marosi, Flame retardancy of fibre-reinforced epoxy resin composites for aerospace applications, *Polymer Degradation and Stability,* **96**, 2011, pp. 371-376 (doi: 10.1016/j.polymdegradstab.2010.03.021).
[21] D.N. Markatos, K.I. Tserpes, E. Rau, K. Brune and Sp. Pantelakis, Degradation of Mode-I Fracture Toughness of CFRP Bonded Joints Due to Release Agent and Moisture Pre-Bond Contamination, *The Journal of Adhesion,* **90**, 2014, pp. 156-173 (doi: 10.1080/00218464.2013.770720).